Materials International
Open Access Journal (ISSN: 2668-5728)

Article
Volume 7, Issue 2, 2025, 16
https://doi.org/10.33263/Materials72.016

Graphene Quantum Dots as Molecular Logic Gates, with Memory and an 8-bit Register

Pradip Shit [1], Asoke P. Chattopadhyay [2]

[1] Department of Chemistry, University of Kalyani, Kalyani 741235, India; pradipshit94@gmail.com (P.S.); asoke@klyuniv.ac.in (A.P.C.);
* Correspondence: asoke@klyuniv.ac.in (A.P.C.);

Received: 26.02.2024; Accepted: 6.10.2024; Published: 10.06.2025

Abstract: Graphene quantum dots (GQDs), prepared in a robust manner, show high fluorescence and are pH dependent. This is used to create logic gates, where appropriate pH control produces a desired fluorescence output above or below a threshold. This is further utilized to produce an implied gate and a memory element with cyclic erase-read-write-read ability. This leads to a regular 8-bit register that can be used as needed.

Keywords: graphene quantum dot; fluorescence; pH dependence; logic gate; memory element; 8-bit register.

1. Introduction

As typical fluorescent materials, GQDs are particularly important for their outstanding optical properties [1-5], superior biocompatibility, and attractive interfacial properties [6-8]. Low biotoxicity and high stability make GQDs ideal photoluminescent (PL) materials in fluorescent bioimaging. GQDs have also found applications as fluorescence probes, drug delivery agents, light-emitting diodes, photocatalysts, supercapacitors, lithium-ion batteries, and environmental issues [9-12].

The computer industry continues to deliver faster processors with larger memory and electronic circuits with higher chip density and computational power. A molecule can change its properties depending on its environment. In computers, information processing is ultimately based on Boolean algebra. In this two-state logic framework, variables can assume only one of two values (1 or 0) at a given time. Using this, de Silva et al. developed a molecular logic device (AND logic gate) three decades ago [13]. Since then, researchers have designed different molecular logic gates, such as YES [14,15], NOT [15], AND [14-19], OR [15], NOR [15,20-22], IMPLY [16,23-26], INHIBIT [14,15,22,23,25-27], XOR [14,15], XNOR [28] and more advanced ones e.g. half-adder, decoder, encoder, RS flip-flop, demultiplexer etc. [14]. Therefore, advances in molecular logic devices (MLD) and molecular integrated circuits (MIC) may soon lead to molecular computational technologies.

Computer and electronic gadgets have been significantly miniaturized and highly efficient due to the development of silicon-based microprocessors. Data storage and protection are two major aspects of information technology. For efficient data use, storage devices with high “write-read-erase” speeds are needed in the future. Silicon-based devices have nearly reached the limit due to physical, technological, and economic constraints. Therefore,

molecular storage devices are probably the way forward instead of semiconductor devices [29,30].

Recently, a molecular keypad lock has also been designed. The most important feature of such a system is the dependence of the output signal on the proper combination and the correct order of input signals. Thus, the keypad lock can defend the system against illegal invasion by unauthorized users. Such molecular devices, capable of authorizing password-based access, are significant for information protection at the molecular scale. Despite the novelty and importance, only a few systems are qualified for such chemical password-based access to date [14].

Currently, graphene-based materials are produced by conventional physical and chemical methods, including micromechanical cleavage [31,32], reduction of exfoliated graphene oxide (GO) [33], and solvothermal synthesis [34]. We synthesized GQDs through modification of a known process viz. pyrolysis of citric acid [35]. These were characterized in the usual manner and used to create logic gates, from which more complicated gates and an erasable password-protected write-read-erase system have been designed. The system is easy to prepare, robust, and the output is pH-dependent. It is also reversible. In other words, a simple change in pH can alter the output. However, such a system can also produce a password-based lock, as demonstrated later in this work.

2. Materials and Methods

2.1. Materials.

Citric acid was purchased from S. D. Fine Chemicals (Delhi, India). Sodium hydroxide pellets and Tris buffer were purchased from Sigma Aldrich (India). All reagents were of AR grade and were used as received without further purification.

2.2. Synthesis of graphene quantum dots.

Graphene quantum dots were synthesized from citric acid by pyrolysis following a previously used procedure [35]. Briefly, 2 g citric acid was put into a beaker and heated to 200 ºC using a heating mantle. The solid melts about 5 min later. Subsequently, the color of the liquid changes from colorless to pale yellow, then to orange after 30 min, indicating the formation of GQDs. The orange liquid was added drop by drop into 100 mL of 10 mg/mL NaOH solution under vigorous stirring. After the pH was neutralized to 7, an aqueous solution of GQDs was obtained.

2.3. Characterization of graphene quantum dots.

The graphene quantum dots were characterized by powder X-ray diffraction (PXRD), FT-IR spectroscopy, transmission electron microscopy (TEM), UV-Vis spectrophotometry, and fluorimetry. PXRD was carried out in a Bruker D8 Advance instrument, with monochromatic X-ray from Cu-Kα radiation (λ=1.5418 Å), from 10° to 80° at a scanning rate of 0.02^0 per second. FT-IR spectra were obtained with a Perkin Elmer L120-000A spectrometer. TEM images were obtained in a Tecnai T20 instrument. For this, a drop of the solution was taken on a carbon-coated Cu grid, which was dried in a vacuum. UV-Vis spectra were recorded on a Shimadzu UV-2450 spectrophotometer between 190 and 700 nm. Fluorescence was examined in a Shimadzu spectrofluorimeter between 400 and 650 nm, with

excitation at 360 nm. Both UV-Vis and fluorescence spectra were taken with 10 μL GQD solution in 2 mL 10 mM Tris buffer solution. The pH of the medium was adjusted with 0.1 M NaOH and 0.1 M HCl solutions.

3. Results and Discussion

TEM and HRTEM images of GQDs are shown in Figure 1 (a) and (b), respectively. The GQDs are mostly around 5 nm in size. FTIR spectra of GQDs are shown in Figure 2, where the prominent bands are at 3409, 1649, 1574, 1386, and 1078 cm^{-1}. These correspond to OH, C=O, C=C, COOH, and C-O vibrations. The powder XRD pattern of GQDs is shown in Figure 3, where a peak around 25° is the signature of the (002) peak of graphene, rGO, and GQD. The UV-Vis spectrum of the GQD solution is shown in Figure 4(a), with λmax at 360 nm. The fluorescence spectrum of the GQD solution is shown in Figure 4(b), where a prominent emission at 460 nm is seen. Figure 5 shows how this fluorescence at 460 nm depends on pH, by varying pH from 1.84 to 12.85, when the fluorescence intensity is seen to increase systematically. This is under investigation, but we hypothesize that the fluorescence is due to various -COOH, -COH, -O- and other such groups on the GQD surface, which, again, when fluorescence is switched off.

Figure 1. (a) TEM; **(b)** HRTEM image of GQD nanoparticles.

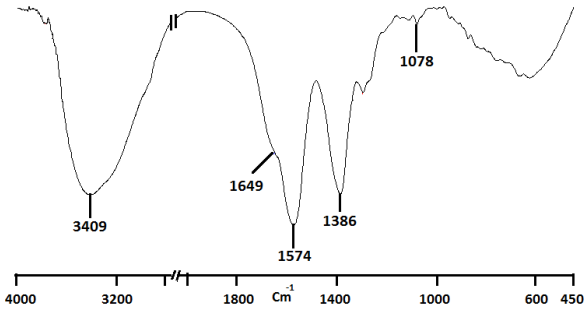

Figure 2. FTIR spectrum of GQD.

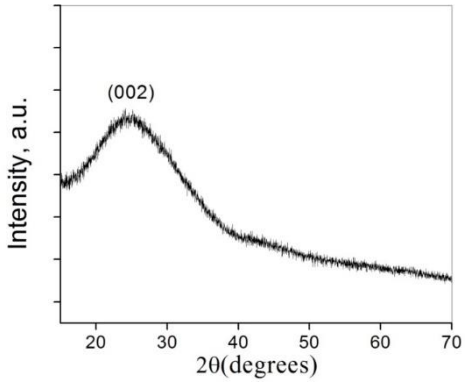

Figure 3. Powder XRD pattern of GQDs.

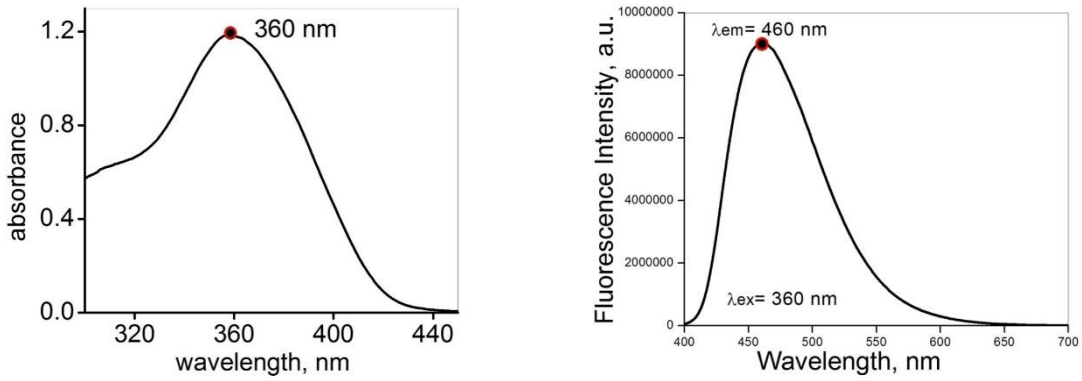

(a) **(b)**

Figure 4. (a) UV-Vis; **(b)** fluorescence spectra of aqueous solution of GQDs. λexc = 360 nm.

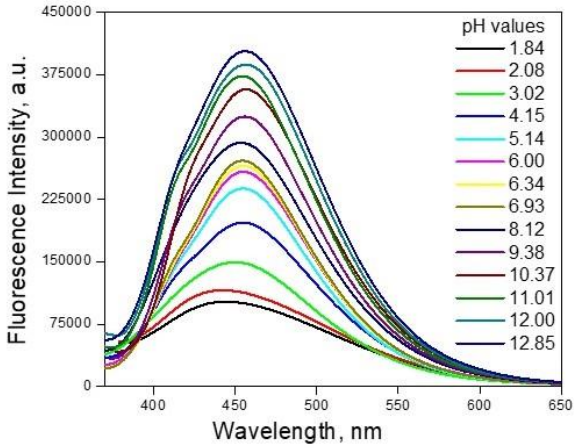

Figure 5. Fluorescence increase of GQD solution from pH 1.84 to 12.85.

3.1. Logic gates.

This is used to build logic gates as follows. Figure 6 shows how a change in the pH of the solution can reversibly switch the fluorescence between "high" and "low" levels. A NOT gate is conceptualized, as shown in Figure 7, whereby the input of H^+, the output (high fluorescence), is turned off. Similarly, with OH^- input, the high fluorescence remains unchanged. This is called a YES gate or a buffer gate, as shown in Figure 8. From here, a suitable combination of inputs leading to a desired output can be easily designed. For example, Fig. 9 shows an IMPLY or IMPLICATION gate, where the output turns off only when H^+ alone is added. In all other possible inputs, the output stays ON (i.e., at high fluorescence at 460 nm). In all these cases, the fluorescence intensity at 460 nm acts as the output.

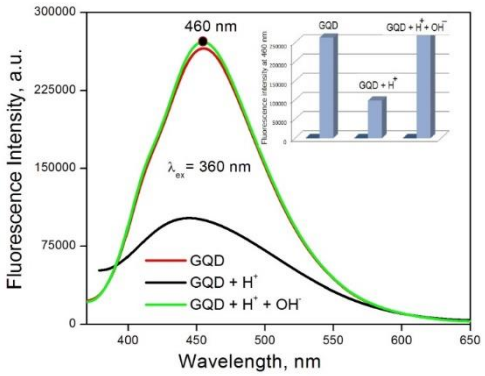

Figure 6. Fluorescence of GQD solution (red) in low (black) and high pH (green). λexc = 360 nm. Inset: Bar plot fluorescence intensity change with pH at 460 nm of GQD solution.

The inputs are H^+ and OH^- ions in suitable concentration and amount. Please note that, in all cases shown, the truth table of the gates is also given, where 1 and 0 on the input side mean whether a particular input (H^+ and/or OH^- ions) is added or not. Similarly, on the output side, 1 and 0 stand for whether the fluorescence intensity at 460 nm of the GQD solution is high or low.

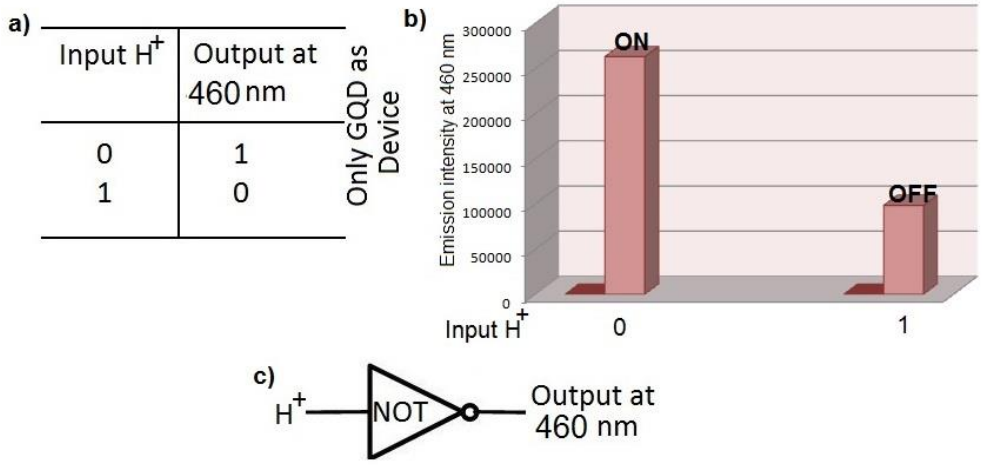

Figure 7. NOT logic gate, with **(a)** truth table; **(b)** optical response based on fluorescence intensity at 460 nm with input as H^+; **(c)** schematic representation of the gate.

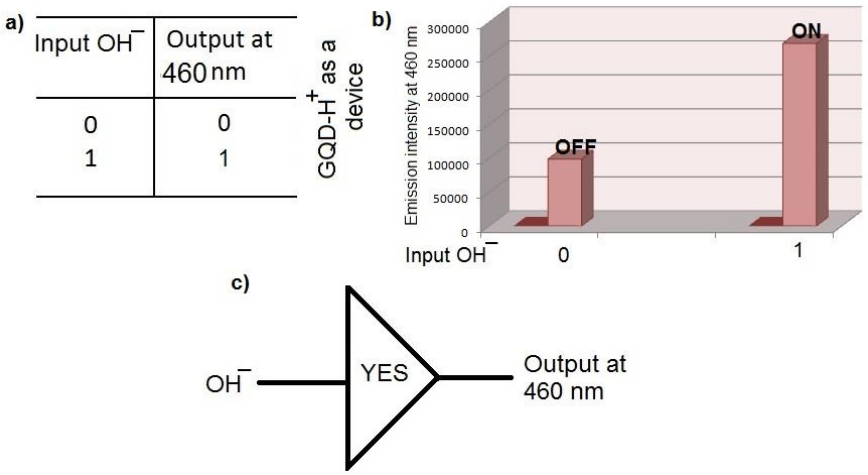

Figure 8. YES logic gate with **(a)** truth table; **(b)** optical response based on 460 nm with OH^- as input to GQD–H^+as device; **(c)** schematic representation of the gate.

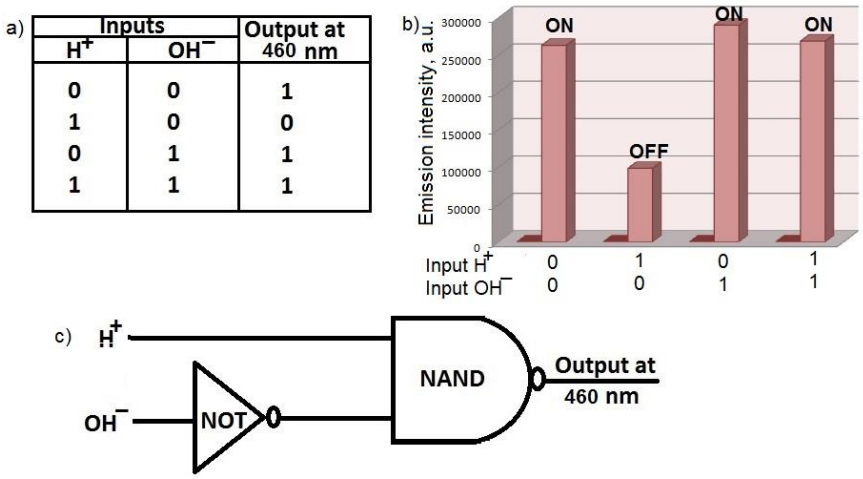

Figure 9. IMPLICATION logic gate with GQDs as device and H^+, OH^- as dual input. **(a)** truth table; **(b)** optical response at 460 nm; **(c)** schematic representation.

3.2. Memory element.

With the above convention, a sequential logic circuit has been designed, as shown in Figure 10(a). The actual operations are shown in Figure 10(b). Let us suppose the current output is 1 (high fluorescence). This can be read, then erased (i.e., low fluorescence) with the addition of H^+ input and turned back on again with OH- input. The set and reset parameters depend on how we set up this unit, which can act as an erasable writeable memory element. The fluorescence intensity of the GQD solution at 460 nm, when excited at 360 nm, is shown in Fig. 5 and represented in the bar diagram in Figure 11. This can be used to represent numbers in the octal system. For example, the intensities at pH 1.84 to 12.85 can be designated as 0, 1, 2, 7. Then, the set of fluorescence intensities, shown in Figure 12, can represent numbers 13207465 in octal and 2953013 in decimal, respectively. The arrangement is as shown in Figure 13, where one can have a cuvette in front of each of the 8 readers. One can also have data from P1 to P4 representing characters and P5 to P8 numerals or any such combination. We can think of a diode array (or similar device) that can identify fixed-intensity emission. Then we have an 8-bit register essentially. We can use it to read, write, store, and erase data.

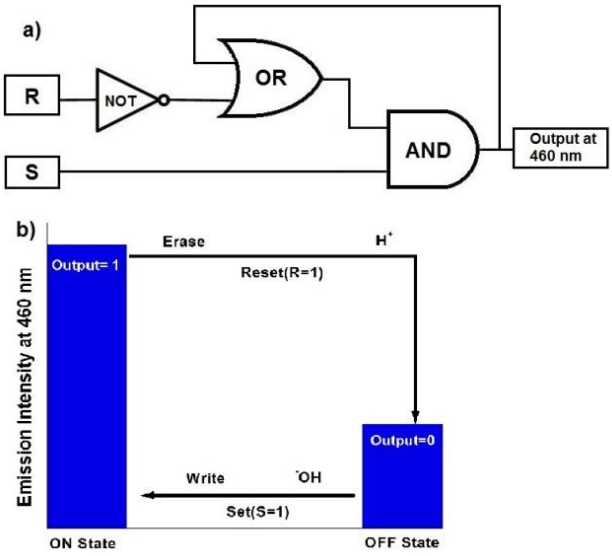

Figure 10. (a) Sequential logic circuit with two inputs (H^+, OH^-) and output at 460 nm; **(b)** schematic representation of "Read-Erase-Write" operations in the memory element.

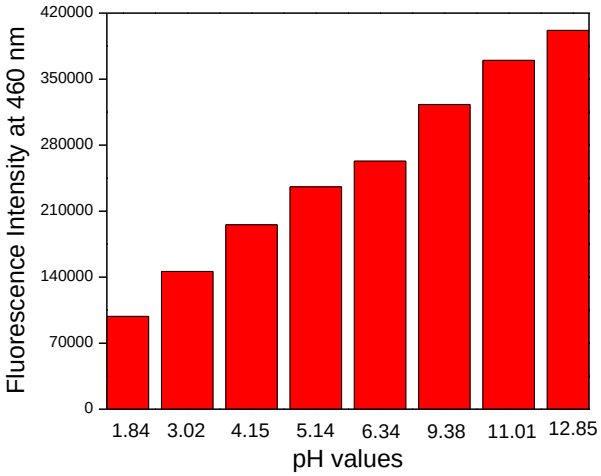

Figure 11. Bar representation of fluorescence intensity of GQDs at 460 nm at different pH values where λ_{ex}= 360 nm.

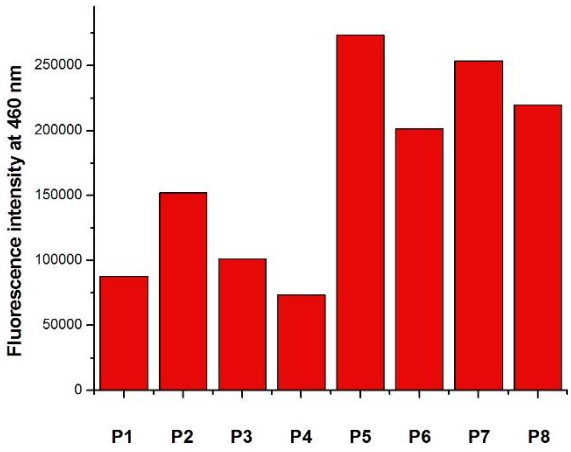

(a)

Value in Octal	**1**	**3**	**2**	**0**	**7**	**4**	**6**	**5**
Value in Decimal	**0**	**2**	**9**	**5**	**3**	**0**	**1**	**3**

(b)

Figure 12. (a) Fluorescent intensities of different cuvettes at 460 nm; **(b)** corresponding value in octal and decimal representations.

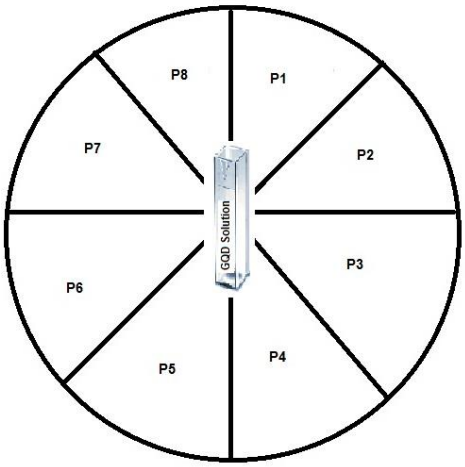

Figure 13. Schematic 8-bit register with "readers" P1 to P8, the cuvette at the center. The light source, shutters on P1 – P8, and how they are operated are not shown.

3.4. Password system.

The above concept is developed in Figure 13, where 8 "readers" are placed. These are marked P1 to P8 as before. There is a cuvette at the center. Normally, the "readers" have shutters/guards around them. When a shutter is opened, say from P6, it can sense the emission intensity at the center (where the GQD solution is in a cuvette). Suppose it reads the intensity as 7. The shutter is put on P6 again, and the GQD solution is suitably modified (H^+ or OH^- added to it), and another shutter, say from P7, is opened. It reads 4 now. One can also have 8 cuvettes, suitably shuttered, before the 8 "readers", the pH of which can be controlled via valves/switches. After a sequence is successfully read, the corresponding number/letter is sent to a central processor, which performs the required action.

The scheme presented in Figures 11, 12, and 13 differs in principle from most of the logic gates found in literature. There have been reports of multi-valued output being used as comparators [36-38]. There are also reports of 4 input systems, etc. [39]. However, they involve the use of complicated biomolecules such as K-Ras and miRNA. In most cases, the probe switches between two states. Some examples include fairly large molecules, which require

substantial synthetic effort to produce and ultimately yield binary output via intricate photophysical processes. Some such examples may be found here [40]. Other works contain molecules with inputs but outputs in different wavelengths [41,42]. While an interesting 4-state system has been proposed combining sequential and combinational operations in a single unit [43], this also entails the synthesis of a rather complicated macrocycle and its switching behavior, including the effects of inputs. The system shown in the present work consists of a simple solution of GQDs, with inputs H^+ and OH^-. This is shown to create a choice of 8 states, i.e., a full-fledged octal register/counter. We are currently investigating whether other carbon-based nanomaterials can lead to such simple multi-valued combinatorics.

4. Conclusions

The GQD solution, synthesized by a known process, exhibits fluorescence at 460 nm upon excitation at 360 nm. The fluorescence intensity is high in an alkaline solution but is quenched in acidic conditions. pH-dependent fluorescence of GQD solution is used to design simple logic gates, an erasable writeable memory element, and an 8-bit register. One can use the 8-bit register for various purposes. H^+ and OH^- ions act as chemical inputs, and emission intensity at 460 nm is the output. We have shown/suggested how all this is possible with the GQD solution, an acid, and an alkali. Of course, one needs to integrate these with more sophisticated elements for proper implementation of the idea.

Funding

This research received no external funding.

Acknowledgments

The authors wish to acknowledge the help and assistance received from Prof. K. Ghosh and Dr. R. Raza of the Chemistry Department KU. PS gratefully acknowledges support from KU in the form of URS.

Conflicts of Interest

The authors declare no conflict of interest.

References

1. Cui, Y.; Liu, L.; Shi, M.; Wang, Y.; Meng, X.; Chen, Y.; Huang, Q.; Liu, C. A Review of Advances in Graphene Quantum Dots: From Preparation and Modification Methods to Application. *J. Carbon Res*. **2024**, *10*, 7, https://doi.org/10.3390/c10010007.
2. Ghaffarkhah, A.; Hosseini, E.; Kamkar, M.; Sehat, A.A.; Dordanihaghighi, S.; Allahbakhsh, A.; van der Kuur, C.; Arjmand, M. Synthesis, Applications, and Prospects of Graphene Quantum Dots: A Comprehensive Review. *Small* **2022**, *18*, 2102683, https://doi.org/10.1002/smll.202102683.
3. Yang, S.; Sun, J.; Li, X.; Zhou, W.; Wang, Z.; He, P.; Ding, G.; Xie, X.; Kang, Z.; Jiang, M. Large-scale fabrication of heavy doped carbon quantum dots with tunable-photoluminescence and sensitive fluorescence detection. *J. Mater. Chem. A* **2014**, *2*, 8660-8667, https://doi.org/10.1039/C4TA00860J.
4. Barrati, F.; Avatefi, M.; Mahmoudifard, M. A review of graphene quantum dots and their potential biomedical applications. *J. Eng. Fibers Fabrics* **2023**, *37*, 1137-1158, https://doi.org/10.1177/08853282221125311.

5. Zhang, P.; Zhao, X.; Ji, Y.; Ouyang, Z.; Wen, X.; Li, J.; Su, Z.; Wei, G. Electrospinning graphene quantum dots into a nanofibrous membrane for dual-purpose fluorescent and electrochemical biosensors. *J. Mater. Chem. B* **2015**, *3*, 2487-2496, https://doi.org/10.1039/C4TB02092H.
6. Wang, G.; Guo, Q.; Chen, D.; Liu, Z.; Zheng, X.; Xu, A.; Yang, S.; Ding, G. Facile and Highly Effective Synthesis of Controllable Lattice Sulfur-Doped Graphene Quantum Dots via Hydrothermal Treatment of Durian. *ACS Appl. Mater. Interfaces* **2018**, *10*, 5750-5759, https://doi.org/10.1021/acsami.7b16002.
7. Zhao, C.; Song, X.; Liu, Y.; Fu, Y.; Ye, L.; Wang, N.; Wang, F.; Li, L.; Mohammadniaei, M. Synthesis of graphene quantum dots and their applications in drug delivery. *J. Nanobiotech*. **2020**, *18*, 142, https://doi.org/10.1186/s12951-020-00698-z.
8. Son, D.I.; Kwon, B.W.; Park, D.H.; Seo, W.S.; Yi, Y.; Angadi, B.; Lee, C.L.; Choi, W.K. Emissive ZnO-graphene quantum dots for white-light-emitting diodes. *Nat. Nanotechnol.* **2012**, *7*, 465−471, https://doi.org/10.1038/nnano.2012.71.
9. Kovalchuk, A.; Huang, K.; Xiang, C.; Martí, A.A.; Tour, J.M. Luminescent Polymer Composite Films Containing Coal-Derived Graphene Quantum Dots. *ACS Appl. Mater. Interfaces* **2015**, *7*, 26063-26068, https://doi.org/10.1021/acsami.5b06057.
10. Biswas, M.C.; Islam, Md.T.; Nandy, P.K.; Hossain, Md.M. Graphene Quantum Dots (GQDs) for Bioimaging and Drug Delivery Applications: A Review. *ACS Mater. Lett.* **2021**, *3*, 889-911, https://doi.org/10.1021/acsmaterialslett.0c00550.
11. Konstantatos, G.; Badioli, M.; Gaudreau, L.; Osmond, J.; Bernechea, M.; De Arquer, F.P.G.; Gatti, F.; Koppens, F.H.L. Hybrid graphene-quantum dot phototransistors with ultrahigh gain. *Nat. Nanotechnol.* **2012**, *7*, 363-368, https://doi.org/10.1038/nnano.2012.60.
12. Facure, M.H.M.; Schneider, R.; Mercante, L.A.; Correa, D.S. A review on graphene quantum dots and their nanocomposites: from laboratory synthesis towards agricultural and environmental applications. *Environ. Sci.: Nano* **2020**, *7*, 3710-3734, https://doi.org/10.1039/D0EN00787K.
13. de Silva, P.A.; Gunaratne, H.Q.N.; McCoy, C.P. A molecular photoionic AND gate based on fluorescent signalling. *Nature* **1993**, *364*, 42-44, https://doi.org/10.1038/364042a0.
14. Yao, C.Y.; Lin, H.Y.; Crory, H.S.N.; de Silva, A.P. Supra-molecular agents running tasks intelligently (SMARTI): recent developments in molecular logic-based computation. *Mol. Syst. Des. Eng.* **2020,** *5*, 1325-1353, https://doi.org/10.1039/D0ME00082E.
15. Jiang, T.; Teng, Y.; Li, C.; Gan, Q.; Zhang, J.; Zou, Y.; Desai, B.K.; Yan, Y. Establishing Tunable Genetic Logic Gates by Varying Regulatory Parameters. *ACS Syth. Biol.* **2023**, *12*, 3730-3742, https://doi.org/10.1021/acssynbio.3c00554.
16. Chen, M.; Wang, C.; Ding, Z.; Wang, H.; Wang, Y.; Liu, Z. A Molecular Logic Gate for Developing AND Logic Probes and the Application in Hepatopathy Differentiation. *ACS Central Sci*. **2022**, *8*, 837-844, https://doi.org/10.1021/acscentsci.2c00387.
17. Magri, D.C.; Brown, D.J.; McClean, G.D.; de Silva, A.P. Communicating Chemical Congregation: A Molecular AND Logic Gate with Three Chemical Inputs as a "Lab-on-a-Molecule" Prototype. *J. Am. Chem. Soc.* **2006**, *128*, 4950-4951, https://doi.org/10.1021/ja058295+.
18. Jiang, S.; Mao, W.; Mao, D.; Li, Z.T.; Ma, D. AND molecular logic gates based on host-guest complexation operational in live cells. *Chin. Chem. Lett.* **2022**, *33*, 881-884, https://doi.org/10.1016/j.cclet.2021.08.021.
19. Zhang, N.; Lo, W.Y.; Jose, A.; Cai, Z.; Li, L.; Yu, L. A Single-Molecular AND Gate Operated with Two Orthogonal Switching Mechanisms. *Adv. Mater.* **2017**, *29*, 1701248, https://doi.org/10.1002/adma.201701248.
20. Maiti, S.S.; Chall, S.; Bhattacharya, S.C. Aggregation-Induced Fabrication of Fluorescent Organic Nanorings: Selective Biosensing of Cysteine and Application to Molecular Logic Gate. *Langmuir* **2015**, *31*, 5025-5032, https://doi.org/10.1021/acs.langmuir.5b00154.
21. Soe, W.H.; Manzano, C.; Renaud, N.; de Mendoza, P.; De Sarkar, A.; Ample, F.; Hliwa, M.; Echavarren, A.M.; Chandrasekhar, N.; Joachim, C. Manipulating Molecular Quantum States with Classical Metal Atom Inputs: Demonstration of a Single Molecule NOR Logic Gate. *ACS Nano* **2011**, *5*, 1436-1440, https://doi.org/10.1021/nn1033899.
22. Zanella, S.; Hernandez-Rodriguez, M.A.; Ferreira, R.A.S.; Brites, C.D.S. Lanthanide-based logic: a venture for the future of molecular computing. *Chem. Commun*. **2023**, *59*, 7863-7874, https://doi.org/10.1039/D3CC01827J.
23. Prabakaran, G.; Velmurugan, K.; Vickram, R.; David, C.I.; Thamilselvan, A.; Prabhu, J.; Nandhakumar, R. Triphenyl-imidazole based reversible coloro/fluorimetric sensing and electrochemical removal of Cu^{2+} ions

using capacitive deionization and molecular logic gates. *Spectrochim. Acta A Mol. Biomol. Spectrosc*. **2021**, *246*, 119018, https://doi.org/10.1016/j.saa.2020.119018.

24. Zhang, Z.; Zhou, R.; Dong, Y.; Song, M.; Tian, L.; Zhao, Z. An indicator displacement assay-based optical chemosensor for heparin with a dual-readout and a reversible molecular logic gate operation based on the pyranine/methyl viologen. *Biosens. Bioelectron*. **2021**, *194*, 113612, https://doi.org/10.1016/j.bios.2021.113612.
25. He, X.; Xie, Q.; Fan, J.; Xu, C.; Xu, W.; Li, Y.; Ding, F.; Deng, H.; Chen, H.; Shen, J. Dual-functional chemosensor with colorimetric/ratiometric response to Cu(II)/Zn(II) ions and its applications in bioimaging and molecular logic gates. *Dyes Pigm.* **2020**, *177*, 108255, https://doi.org/10.1016/j.dyepig.2020.108255.
26. Trifoi, L.A.; Hodgson, G.K.; Dogantzis, N.P.; Impellizzeri, S. A Reconfigurable, Dual-Output INHIBIT and IMPLICATION Molecular Logic Gate. *Front. Chem.* **2020**, *8*, 470, https://doi.org/10.3389/fchem.2020.00470.
27. George, N.; Saini, P.; Singh, G.; Singh, R.; Singh, G.; Malik, P.; Singh, H.; Kaur, G.; Singh, J. Detection of copper in tea and water sample: A click-oriented azomethine-based 1,2,3-triazole fluorescent chemosensor with reversible INHIBIT logic gate behavior and computational aspects. *J. Mol. Struct*. **2024**, *1311*, 138288, https://doi.org/10.1016/j.molstruc.2024.138288.
28. Hwang, J.; Joh, H.; Kim, C.; Ahn, J.; Jeon, S. Monolithically Integrated Complementary Ferroelectric FET XNOR Synapse for the Binary Neural Network. *ACS Appl. Mater. Interf*. **2024**, *16*, 2467-2476, https://doi.org/10.1021/acsami.3c13945.
29. Bao, L.; Huang, L.; Guo, H.; Gao, H-J. Construction and physical properties of low-dimensional structures for nanoscale electronic devices. *Phys. Chem. Chem. Phys*. **2022**, *24*, 9082-9117, https://doi.org/10.1039/D1CP05981E.
30. Lian, H.; Chen, X.; Hao, H.; Han, J.; Lau, M-T.; Li, Z.; Zhou, Z.; Dong, Q.; Wang, W-Y. Metal-containing organic compounds for memory and data storage applications. *Chem. Soc. Rev*. **2022**, *51*, 1926-1982, https://doi.org/10.1039/D0CS00569J.
31. Novoselov, K.S.; Geim, A.K.; Morozov, S.V.; Jiang, D.; Zhang, Y.; Dubonos, S.V.; Grigorieva, I.V.; Firsov, A.A. Electric Field Effect in Atomically Thin Carbon Films. *Science* **2004**, *306*, 666-669, https://doi.org/10.1126/science.1102896.
32. Pan, D.; Zhang, J.; Li, Z.; Wu, M. Hydrothermal Route for Cutting Graphene Sheets into Blue-Luminescent Graphene Quantum Dots. *Adv. Mater*. **2010**, *22*, 734-738, https://doi.org/10.1002/adma.200902825.
33. Li, D.; Müller, M.B.; Gilje, S.; Kaner, R.B.; Wallace, G.G. Processable aqueous dispersions of graphene nanosheets. *Nat. Nanotech.* **2008**, *3*, 101, https://doi.org/10.1038/nnano.2007.451.
34. Choucair, M.; Thordarson, P.; Stride, J.A. Gram-scale production of graphene based on solvothermal synthesis and sonication. *Nat. Nanotech*. **2009**, *4*, 30, https://doi.org/10.1038/nnano.2008.365.
35. Dong, Y.; Shao, J.; Chen, C.; Li, H.; Wang, R.; Chi, R.; Lin, X.; Chen, G. Blue luminescent graphene quantum dots and graphene oxide prepared by tuning the carbonization degree of citric acid. *Carbon* **2012**, *50*, 4738-4743, https://doi.org/10.1016/j.carbon.2012.06.002.
36. Georgiev, N.I.; Yaneva, I.S.; Surleva, A.R.; Asiri, A.M.; Bojinov, V.B. Synthesis, sensor activity and logic behavior of a highly water-soluble naphthalimide derivative. *Sens. Actuators B Chem*. **2013**, *184*, 54-63, https://doi.org/10.1016/j.snb.2013.04.066.
37. Georgiev, N.I.; Dimitrova, M.D.; Krasteva, P.V.; Bojinov, V.B. A novel water-soluble 1,8-naphthalimide as a fluorescent pH-probe and a molecular logic circuit. *J. Luminesc*. **2017**, *187*, 383-391, https://doi.org/10.1016/j.jlumin.2017.03.049.
38. Georgiev, N.I.; Bakov, V.V.; Bojinov, V.B. A Tutorial Review on the Fluorescent Probes as a Molecular Logic Circuit—Digital Comparator. *Molecules* **2023**, *28*, 6327, https://doi.org/10.3390/molecules28176327.
39. Liu, L.; Liu, P.; Ga, L.; Ai, J. Advances in Applications of Molecular Logic Gates. *ACS Omega* **2021**, *6*, 30189-30204, https://doi.org/10.1021/acsomega.1c02912.
40. Erbus-Cakmak, S.; Kolemen, S.; Sedgwick, A.C.; Gunnlaugsson, T.; James, T.D.; Yoon, J.; Akkaya, E.U. Molecular logic gates: the past, present and future. *Chem. Soc. Rev*. **2018**, *47*, 2228-2248, https://doi.org/10.1039/C7CS00491E.
41. Tzeli, D.; Petsalakis, I.D.; Theodorakopoulos, G. Molecular logic gates based on benzo-18-crown-6 ether of styrylquinoline: a theoretical study. *Phys. Chem. Chem. Phys*. **2016**, *18*, 32132-32145, https://doi.org/10.1039/C6CP06899E.
42. Bozdemir, O.A.; Guliyev, R.; Buyukcakir, O.; Selcuk, S.; Kolemen, S.; Gulseren, G.; Nalbantoglu, B.H.; Akkaya, E.U. Selective Manipulation of ICT and PET Processes in Styryl-Bodipy Derivatives: Applications

in Molecular Logic and Fluorescence Sensing of Metal Ions. *J. Am. Chem. Soc*. **2010**, *132*, 8029-8036, https://doi.org/10.1021/ja1008163.

43. Daly, B.; Moody, T.S.; Huxley, A.J.M.; Yao, C.; Schazman, B.; Alves-Areias, A.; Malone, J.F.; Gunaratne, H.Q.N.; Nockemann, P.; de Silva, A.P. Molecular memory with downstream logic processing exemplified by switchable and self-indicating guest capture and release. *Nat. Commun*. **2019**, *10*, 49, https://doi.org/10.1038/s41467-018-07902-7.